Stability of Limit Cycles in Hybrid Systems

Ian A. Hiskens
Department of Electrical and Computer Engineering
University of Illinois at Urbana-Champaign
Urbana IL USA
hiskens@ece.uiuc.edu

Abstract

Limit cycles are common in hybrid systems. However the nonsmooth dynamics of such systems makes stability analysis difficult. This paper uses recent extensions of trajectory sensitivity analysis to obtain the characteristic multipliers of nonsmooth limit cycles. The stability of a limit cycle is determined by its characteristic multipliers. The concepts are illustrated using a coupled tank system with on/off valve switching.

1 Introduction

Hybrid systems are characterized by interactions between continuous (smooth) dynamics and discrete events. Such systems are common across a diverse range of application areas. Examples include power systems [1], robotics [2], manufacturing [3] and air-traffic control [4]. In fact, any system where saturation limits are routinely encountered can be thought of as a hybrid system. The limits introduce discrete events which (often) have a significant influence on overall behaviour.

Many hybrid systems exhibit periodic behaviour. Discrete events, such as saturation limits, can act to trap the evolving system state within a constrained region of state space. Therefore even when the underlying continuous dynamics are unstable, the discrete events can induce a stable limit set. Limit cycles (periodic behaviour) are often created in this way. An example is presented in Section 4.

Limit cycles can be stable (attracting), unstable (repelling) or non-stable (saddle). The stability of periodic behaviour is determined by characteristic (or Floquet) multipliers. Characteristic multipliers are a generalization of the eigenvalues at an equilibrium point. A periodic solution corresponds to a fixed point of a Poincaré map. Stability of the periodic solution is the same as the stability of the fixed point. The characteristic multipliers are the eigenvalues of the Poincaré map linearized about the fixed point. It is shown in Section 3 that this linearized map is given by trajectory sensitivities. This paper uses a recent extension of trajectory sensitivity analysis [5] to determine the stability of limit cycles in hybrid systems.

A brief review of hybrid system modelling is given in Section 2. Stability analysis of limit cycles is presented in Section 3, and an example is considered in Section 4. Trajectory sensitivity equations for hybrid systems are provided in the appendix.

2 Model

Deterministic hybrid systems can be represented by a model that consists of differential, switched algebraic, and state-reset (DSAR) equations, i.e.,

$$\dot{\underline{x}} = \underline{f}(\underline{x}, y) \tag{1}$$

$$0 = g^{(0)}(\underline{x}, y) \tag{2}$$

$$0 = \begin{cases} g^{(i-)}(\underline{x}, y) & y_{d,i} < 0 \\ g^{(i+)}(\underline{x}, y) & y_{d,i} > 0 \end{cases} \quad i = 1, ..., d \tag{3}$$

$$\underline{x}^+ = \underline{h}_j(\underline{x}^-, y^-) \qquad y_{e,j} = 0 \quad j \in \{1, ..., e\} \tag{4}$$

where

$$\underline{x} = \begin{bmatrix} x \\ z \\ \lambda \end{bmatrix}, \qquad \underline{f} = \begin{bmatrix} f \\ 0 \\ 0 \end{bmatrix}, \qquad \underline{h}_j = \begin{bmatrix} x \\ h_j \\ \lambda \end{bmatrix}$$

and

- x are the continuous dynamic states,
- z are discrete dynamic states,
- y are algebraic states, and
- λ are parameters.

The model can capture complex behaviour, from hysteresis and non-windup limits through to rule-based

systems [1]. A more extensive presentation of this model is given in [5].

In this model, the parameters λ form part of the extended state $\underline{x}$. This allows a convenient development of trajectory sensitivities. To ensure that parameters remain fixed at their initial values, the corresponding differential equations (1) are defined as $\dot{\lambda} = 0$.

Away from events, system dynamics evolve smoothly according to the familiar differential-algebraic model

$$\dot{\underline{x}} = \underline{f}(\underline{x}, y) \quad (5)$$
$$0 = g(\underline{x}, y) \quad (6)$$

where g is composed of $g^{(0)}$ together with appropriate choices of $g^{(i-)}$ or $g^{(i+)}$, depending on the signs of the corresponding elements of y_d. At switching events (3), some component equations of g change. To satisfy the new $g = 0$ equation, algebraic variables y may undergo a step change. Reset events (4) force a discrete change in elements of z. Algebraic variables may also step at a reset event to ensure $g = 0$ is satisfied with the altered values of z.

The *flows* of $\underline{x}$ and y are defined respectively as

$$\underline{x}(t) = \phi_{\underline{x}}(\underline{x}_0, t) \quad (7)$$
$$y(t) = \phi_y(\underline{x}_0, t) \quad (8)$$

where $\underline{x}(t)$ and $y(t)$ satisfy (1)-(4), along with initial conditions,

$$\phi_{\underline{x}}(\underline{x}_0, t_0) = \underline{x}_0 \quad (9)$$
$$g(\underline{x}_0, \phi_y(\underline{x}_0, t_0)) = 0. \quad (10)$$

Trajectory sensitivities $\Phi_{\underline{x}}$,Φ_y describe the sensitivity of the flows to perturbations in initial conditions $\underline{x}_0$. These sensitivities underlie the linearization of the Poincaré map, and so play a major role in determining the stability of periodic solutions. A summary of the variational equations governing the evolution of these sensitivities is given in the Appendix.

3 Limit Cycle Analysis

Stability of limit cycles is determined using Poincaré maps. A Poincaré map effectively samples the flow of a periodic system once every period. The concept is illustrated in Figure 1. If the limit cycle is stable, oscillations approach the limit cycle over time. The samples provided by the corresponding Poincaré map approach a fixed point. A non-stable limit cycle results in divergent oscillations. The samples of the Poincaré map diverge for such a case.

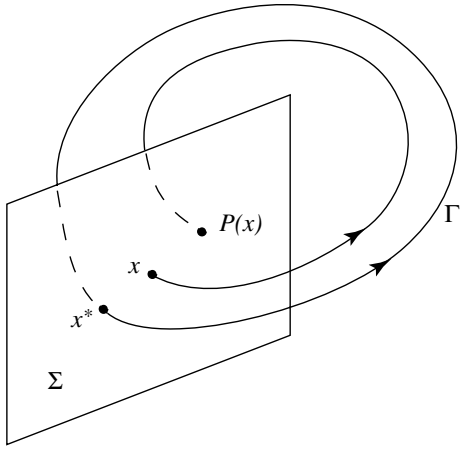

Figure 1: Poincaré map.

To define a Poincaré map, consider the limit cycle Γ shown in Figure 1. Let Σ be a hyperplane transversal to Γ at $\underline{x}^*$. The trajectory emanating from $\underline{x}^*$ will again encounter Σ at $\underline{x}^*$ after T seconds, where T is the minimum period of the limit cycle. Due to the continuity of the flow $\phi_{\underline{x}}$ with respect to initial conditions, trajectories starting on Σ in a neighbourhood of $\underline{x}^*$ will, in approximately T seconds, intersect Σ in the vicinity of $\underline{x}^*$. Hence $\phi_{\underline{x}}$ and Σ define a mapping

$$\underline{x}_{k+1} = P(\underline{x}_k) := \phi_{\underline{x}}(\underline{x}_k, \tau_r(\underline{x}_k)). \quad (11)$$

where $\tau_r(\underline{x}_k) \approx T$ is the time taken for the trajectory to return to Σ. Complete details can be found in [6, 7].

Stability of the Poincaré map (11) is determined by linearizing P at the fixed point $\underline{x}^*$, i.e.,

$$\Delta\underline{x}_{k+1} = DP(\underline{x}^*)\Delta\underline{x}_k. \quad (12)$$

From the definition of $P(\underline{x})$ given by (11), it follows that $DP(\underline{x}^*)$ is closely related to the trajectory sensitivities $\frac{\partial\phi_{\underline{x}}(\underline{x}^*,T)}{\partial\underline{x}_0} \equiv \Phi_{\underline{x}}(\underline{x}^*, T)$. In fact, it is shown in [6] that

$$DP(\underline{x}^*) = \left(I - \frac{\underline{f}(\underline{x}^*, y^*)\sigma^t}{\underline{f}(\underline{x}^*, y^*)^t\sigma}\right)\Phi_{\underline{x}}(\underline{x}^*, T) \quad (13)$$

where σ is a vector normal to Σ.

The matrix $\Phi_{\underline{x}}(\underline{x}^*, T) \equiv \underline{x}_{\underline{x}_0}(T)$ is exactly the trajectory sensitivity matrix after one period of the limit cycle, i.e., starting from $\underline{x}^*$ and returning to $\underline{x}^*$. This matrix is called the *Monodromy matrix*. It is shown in [6] that one eigenvalue of $\Phi_{\underline{x}}(\underline{x}^*, T)$ is always 1, and the corresponding eigenvector lies along $\underline{f}(\underline{x}^*, y^*)$. The remaining eigenvalues of $\Phi_{\underline{x}}(\underline{x}^*, T)$ coincide with the eigenvalues of $DP(\underline{x}^*)$, and are known as the *characteristic multipliers* m_i of the periodic solution. The

characteristic multipliers are independent of the choice of cross-section Σ. Therefore, for hybrid systems, it is often convenient to choose Σ as a triggering hypersurface corresponding to a switching or reset event that occurs along the periodic solution.

Because the characteristic multipliers m_i are the eigenvalues of the linear map $DP(\underline{x}^*)$, they determine the stability of the Poincaré map $P(\underline{x}_k)$, and hence the stability of the periodic solution. Three cases are of importance:

1) All m_i lie within the unit circle, i.e., $|m_i| < 1, \forall i$. The map is stable, so the periodic solution is stable.

2) All m_i lie outside the unit circle. The periodic solution is unstable.

3) Some m_i lie outside the unit circle. The periodic solution is non-stable.

Interestingly, there exists a particular cross-section Σ^*, such that

$$DP(\underline{x}^*)\zeta = \Phi_{\underline{x}}(\underline{x}^*, T)\zeta \tag{14}$$

where $\zeta \in \Sigma^*$. This cross-section Σ^* is the hyperplane spanned by the $n-1$ eigenvectors of $\Phi_{\underline{x}}(\underline{x}^*, T)$ that are not aligned with $\underline{f}(\underline{x}^*, y^*)$. Therefore the vector σ^* that is normal to Σ^* is the left eigenvector of $\Phi_{\underline{x}}(\underline{x}^*, T)$ corresponding to the eigenvalue 1. The hyperplane Σ^* is invariant under $\Phi_{\underline{x}}(\underline{x}^*, T)$, i.e., $\Phi_{\underline{x}}(\underline{x}^*, T)$ maps vectors $\zeta \in \Sigma^*$ back into Σ^*.

4 Example

The two-tank system of Figure 2 can be used to illustrate limit cycles in hybrid systems [8]. The system consists of two tanks and two valves. The first valve adds to the inflow in tank 1, whilst the second valve is a drain valve from tank 2. There is also constant outflow from tank 2 caused by a pump. The system is linearized at a desired operating point.

The objective is to keep the water levels in both tanks within limits using a discrete open/close switching strategy for the valves. The valve associated with tank 1 should open when the level of tank 1 falls to -1, and close when the level of tank 2 goes above 1. The tank 2 valve should open when the level of tank 2 rises to 1, and close when the tank 2 level falls to 0.

Let the water levels of tanks 1 and 2 be given by x_1 and x_2 respectively. The behaviour of x_1 is given by

$\dot{x}_1 = -x_1 - 2$ when tank 1 valve is closed
$\dot{x}_1 = -x_1 + 3$ when tank 1 valve is open.

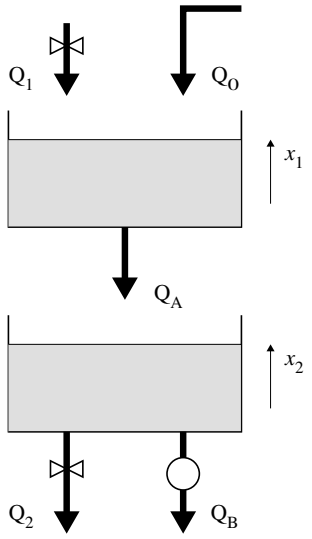

Figure 2: Two-tank example.

Likewise, x_2 is driven by

$\dot{x}_2 = x_1$ when tank 2 valve is closed
$\dot{x}_2 = x_1 - x_2 - 5$ when tank 2 valve is open.

This system can be modelled in the DSAR form as,

$$\begin{aligned}
\dot{x}_1 &= -x_1 + y_1 \\
\dot{x}_2 &= x_1 + y_2 \\
&\left.\begin{aligned} 0 &= y_1 - 3 \\ 0 &= y_3 - x_2 + 1 \end{aligned}\right\} \; y_3 < 0 \\
&\left.\begin{aligned} 0 &= y_1 + 2 \\ 0 &= y_3 - x_1 - 1 \end{aligned}\right\} \; y_3 > 0 \\
&\left.\begin{aligned} 0 &= y_2 + x_2 + 5 \\ 0 &= y_4 + x_2 \end{aligned}\right\} \; y_4 < 0 \\
&\left.\begin{aligned} 0 &= y_2 \\ 0 &= y_4 + x_2 - 1 \end{aligned}\right\} \; y_4 > 0.
\end{aligned}$$

The phase portrait of Figure 3 shows the behaviour of this system for various initial conditions. Trajectories are shown as thin lines. All trajectories approach a stable nonsmooth limit cycle, indicated by the darker line. The limit cycle is shown by itself in Figure 4.

The limit cycle encounters a triggering hypersurface at $x_1 = -1$. (This event corresponds to the tank 1 valve opening.) This surface provides a convenient cross-section Σ for defining a Poincaré map. Consider the point $\underline{x}^* = [-1.0 \quad -0.161]^t$ on the limit cycle immediately after the switching event. Based on this choice for $\underline{x}^*$, the trajectory sensitivities after one period of the limit cycle give,

$$\Phi_{\underline{x}}(\underline{x}^*, T) = \begin{bmatrix} 1.6244 & 2.4977 \\ -0.4337 & -0.7348 \end{bmatrix}$$

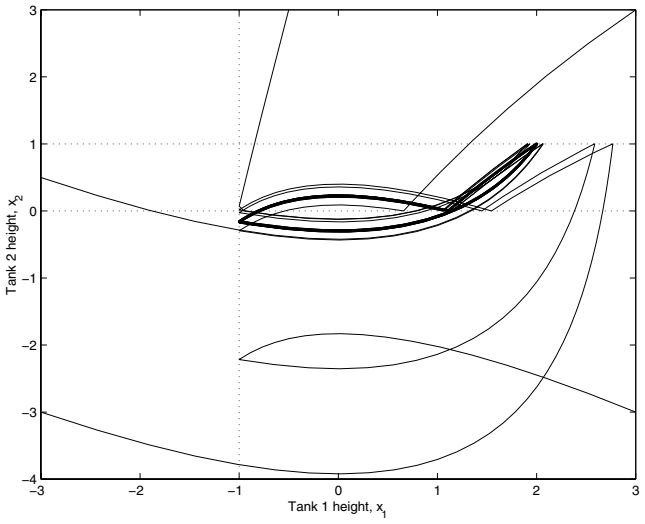

Figure 3: Phase portrait for example.

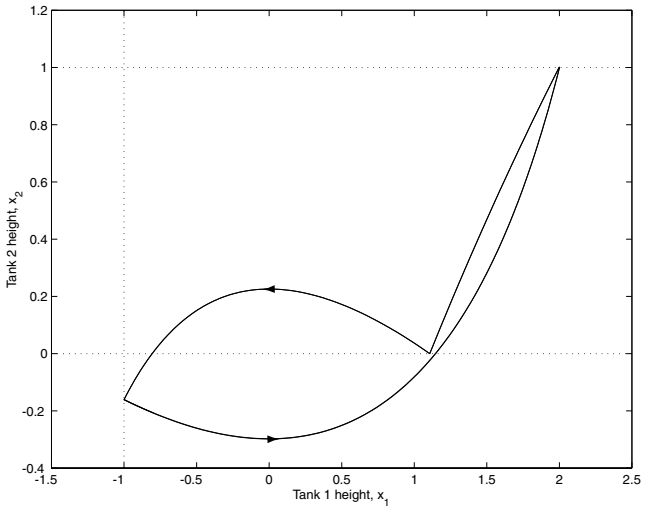

Figure 4: Limit cycle.

which has eigenvalues of 1.0 and -0.1103, and corresponding right eigenvectors

$$ev_1 = \begin{bmatrix} 0.9701 \\ -0.2425 \end{bmatrix}, \qquad ev_2 = \begin{bmatrix} -0.8213 \\ 0.5704 \end{bmatrix}.$$

From the model,

$$\underline{f}(\underline{x}^*, y^*) = \begin{bmatrix} -x_1 + 3 \\ x_1 \end{bmatrix} = \begin{bmatrix} 4 \\ -1 \end{bmatrix}.$$

Notice that $ev_1 = 0.2425\underline{f}(\underline{x}^*, y^*)$. Therefore, as anticipated, the eigenvector corresponding to the unity eigenvalue lies along $\underline{f}(\underline{x}^*, y^*)$. The other eigenvalue, -0.1103, is the characteristic multiplier for this limit cycle. Its magnitude is less than one, proving that the limit cycle is stable.

We shall now confirm that -0.1103 is really an eigenvalue of $DP(\underline{x}^*)$. For the chosen hypersurface $x_1 = -1$, the normal vector is $\sigma = [1 \quad 0]^t$. Therefore from (13),

$$DP(\underline{x}^*) = \begin{bmatrix} 0 & 0 \\ -0.0276 & -0.1103 \end{bmatrix}$$

which has eigenvalues of 0 and -0.1103. When restricted to the hyperplane Σ, the zero eigenvalue disappears, leaving the characteristic multiplier.

Now consider the special cross-section Σ^* that is spanned by ev_2, i.e., the eigenvector of $\Phi_{\underline{x}}(\underline{x}^*, T)$ that is not aligned with $\underline{f}(\underline{x}^*, y^*)$. In this case $\sigma^* = [0.5704 \quad 0.8213]^t$ and

$$DP(\underline{x}^*) = \begin{bmatrix} 0.0621 & 0.2482 \\ -0.0431 & -0.1724 \end{bmatrix}$$

which again has eigenvalues of 0 and -0.1103. Vectors $\zeta \in \Sigma^*$ satisfy

$$0.5704x_1 + 0.8213x_2 = 0$$
$$\Rightarrow \quad x_2 = -0.6945x_1$$

so

$$\begin{aligned} DP(\underline{x}^*)\zeta &= \begin{bmatrix} 0.0621 & 0.2482 \\ -0.0431 & -0.1724 \end{bmatrix} \begin{bmatrix} x_1 \\ -0.6945x_1 \end{bmatrix} \\ &= \begin{bmatrix} -0.1103 \\ 0.0766 \end{bmatrix} x_1 \in \Sigma^* \end{aligned}$$

and

$$\begin{aligned} \Phi_{\underline{x}}(\underline{x}^*, T)\zeta &= \begin{bmatrix} 1.6244 & 2.4977 \\ -0.4337 & -0.7348 \end{bmatrix} \begin{bmatrix} x_1 \\ -0.6945x_1 \end{bmatrix} \\ &= \begin{bmatrix} -0.1103 \\ 0.0766 \end{bmatrix} x_1 \in \Sigma^*. \end{aligned}$$

Notice that $DP(\underline{x}^*)\zeta = \Phi_{\underline{x}}(\underline{x}^*, T)\zeta$ for all $\zeta \in \Sigma^*$.

5 Conclusions

Hybrid systems frequently exhibit periodic behaviour. However the nonsmooth nature of such systems complicates stability analysis. Those complications have been addressed in this paper through application of recent extensions to trajectory sensitivity analysis.

Deterministic hybrid systems can be represented by a coupled set of differential, switched algebraic, and state-reset equations. The variational equations describing the evolution of trajectory sensitivities for this model have recently been developed, and are included as an appendix.

Standard Poincaré map results extend naturally to hybrid systems. The Monodromy matrix is obtained by evaluating trajectory sensitivities over one period of the (possibly nonsmooth) cyclical behaviour. One eigenvalue of this matrix is always unity. The remaining eigenvalues are the characteristic multipliers of the periodic solution. Stability is ensured if all multipliers lie inside the unit circle. Instability occurs if any multiplier lies outside the unit circle.

Acknowledgements

The author wishes to acknowledge the support of the Australian Research Council through the project grant "Analysis and Assessment of Voltage Collapse", the EPRI/DoD Complex Interactive Networks/Systems Initiative, and the Grainger Foundation.

References

[1] I.A. Hiskens and M.A. Pai, "Hybrid systems view of power system modelling," in *Proceedings of the IEEE International Symposium on Circuits and Systems*, Geneva, Switzerland, May 2000.

[2] M.H. Raibert, *Legged Robots That Balance*, MIT Press, Cambridge, MA, 1986.

[3] S. Pettersson, "Analysis and design of hybrid systems," Ph.D. Thesis, Department of Signals and Systems, Chalmers University of Technology, Göteborg, Sweden, 1999.

[4] C. Tomlin, G. Pappas, and S. Sastry, "Conflict resolution for air traffic management: A study in multiagent hybrid systems," *IEEE Transactions on Automatic Control*, vol. 43, no. 4, pp. 509–521, April 1998.

[5] I.A. Hiskens and M.A. Pai, "Trajectory sensitivity analysis of hybrid systems," *IEEE Transactions on Circuits and Systems I*, vol. 47, no. 2, pp. 204–220, February 2000.

[6] T.S Parker and L.O. Chua, *Practical Numerical Algorithms for Chaotic Systems*, Springer-Verlag, New York, NY, 1989.

[7] R. Seydel, *Practical Bifurcation and Stability Analysis*, Springer-Verlag, New York, 2nd edition, 1994.

[8] M. Rubensson, B. Lennartsson, and S. Pettersson, "Convergence to limit cycles in hybrid systems - an example," in *Preprints of 8th International Federation of Automatic Control Symposium on Large Scale Systems: Theory & Applications*, Rio Patras, Greece, 1998, pp. 704–709.

A Trajectory Sensitivity Equations

The sensitivity of the flows $\phi_{\underline{x}}$ and ϕ_y to initial conditions $\underline{x}_0$ are obtained by linearizing (7),(8) about the nominal trajectory,

$$\Delta \underline{x}(t) = \frac{\partial \phi_{\underline{x}}(\underline{x}_0, t)}{\partial \underline{x}_0} \Delta \underline{x}_0 \quad (15)$$

$$\Delta y(t) = \frac{\partial \phi_y(\underline{x}_0, t)}{\partial \underline{x}_0} \Delta \underline{x}_0. \quad (16)$$

The time-varying partial derivative matrices given in (15),(16) are known as *trajectory sensitivities*, and can be expressed in the alternative forms

$$\frac{\partial \phi_{\underline{x}}(\underline{x}_0, t)}{\partial \underline{x}_0} \equiv \underline{x}_{\underline{x}_0}(t) \equiv \Phi_{\underline{x}}(\underline{x}_0, t) \quad (17)$$

$$\frac{\partial \phi_y(\underline{x}_0, t)}{\partial \underline{x}_0} \equiv y_{\underline{x}_0}(t) \equiv \Phi_y(\underline{x}_0, t). \quad (18)$$

The form $\underline{x}_{\underline{x}_0}, y_{\underline{x}_0}$ enables a clearer development of the variational equations describing the evolution of the sensitivities. This development is summarized below. The alternative form $\Phi_{\underline{x}}(\underline{x}_0, t), \Phi_y(\underline{x}_0, t)$ highlights the connection between the sensitivities and the underlying flows.

Away from events, where system dynamics evolve smoothly, trajectory sensitivities $\underline{x}_{\underline{x}_0}$ and $y_{\underline{x}_0}$ are obtained by differentiating (5),(6) with respect to $\underline{x}_0$. This gives

$$\dot{\underline{x}}_{\underline{x}_0} = \underline{f}_{\underline{x}}(t)\underline{x}_{\underline{x}_0} + \underline{f}_y(t) y_{\underline{x}_0} \quad (19)$$

$$0 = g_{\underline{x}}(t)\underline{x}_{\underline{x}_0} + g_y(t) y_{\underline{x}_0} \quad (20)$$

where $\underline{f}_{\underline{x}} \equiv \partial \underline{f} / \partial \underline{x}$, and likewise for the other Jacobian matrices. Note that $\underline{f}_{\underline{x}}$, $\underline{f}_y$, $g_{\underline{x}}$, g_y are evaluated along the trajectory, and hence are time varying matrices. It is shown in [5] that the solution of this (potentially high order) DA system can be obtained as a by-product of solving the original DA system (5),(6).

Initial conditions for $\underline{x}_{\underline{x}_0}$ are obtained from (9) as

$$\underline{x}_{\underline{x}_0}(t_0) = I$$

where I is the identity matrix. Initial conditions for $y_{\underline{x}_0}$ follow directly from (20),

$$0 = g_{\underline{x}}(t_0) + g_y(t_0) y_{\underline{x}_0}(t_0).$$

Equations (19),(20) describe the evolution of the sensitivities $x_{\underline{x}_0}$ and $y_{\underline{x}_0}$ between events. However at an event, the sensitivities are generally discontinuous. It is necessary to calculate *jump conditions* describing the step change in $x_{\underline{x}_0}$ and $y_{\underline{x}_0}$. For clarity, consider a single switching/reset event, so the model (1)-(4) reduces to the form

$$\dot{\underline{x}} = \underline{f}(\underline{x}, y) \tag{21}$$

$$0 = \begin{cases} g^-(\underline{x}, y) & s(\underline{x}, y) < 0 \\ g^+(\underline{x}, y) & s(\underline{x}, y) > 0 \end{cases} \tag{22}$$

$$\underline{x}^+ = \underline{h}(\underline{x}^-, y^-) \qquad s(\underline{x}, y) = 0. \tag{23}$$

Let $(\underline{x}(\tau), y(\tau))$ be the point where the trajectory encounters the hypersurface $s(\underline{x}, y) = 0$, i.e., the point where an event is triggered. This point is called the *junction point* and τ is the *junction time*.

Just prior to event triggering, at time τ^-, we have

$$\begin{aligned} \underline{x}^- = \underline{x}(\tau^-) &= \phi_{\underline{x}}(\underline{x}_0, \tau^-) \\ y^- = y^-(\tau^-) &= \phi_y(\underline{x}_0, \tau^-) \end{aligned}$$

where

$$g^-(\underline{x}^-, y^-) = 0.$$

Similarly, $\underline{x}^+, y^+$ are defined for time τ^+, just after the event has occurred. It is shown in [5] that the jump conditions for the sensitivities $\underline{x}_{\underline{x}_0}$ are given by

$$\underline{x}_{\underline{x}_0}(\tau^+) = \underline{h}^*_{\underline{x}}\, \underline{x}_{\underline{x}_0}(\tau^-) - \left(\underline{f}^+ - \underline{h}^*_{\underline{x}}\, \underline{f}^-\right) \tau_{\underline{x}_0} \tag{24}$$

where

$$\begin{aligned} \underline{h}^*_{\underline{x}} &= \left(\underline{h}_{\underline{x}} - \underline{h}_y (g^-_y)^{-1} g^-_{\underline{x}}\right)\Big|_{\tau^-} \\ \tau_{\underline{x}_0} &= -\frac{\left(s_{\underline{x}} - s_y (g^-_y)^{-1} g^-_{\underline{x}}\right)\Big|_{\tau^-} \underline{x}_{\underline{x}_0}(\tau^-)}{\left(s_{\underline{x}} - s_y (g^-_y)^{-1} g^-_{\underline{x}}\right)\big|_{\tau^-} \underline{f}^-} \\ \underline{f}^- &= \underline{f}(\underline{x}(\tau^-), y^-(\tau^-)) \\ \underline{f}^+ &= \underline{f}(\underline{x}(\tau^+), y^+(\tau^+)). \end{aligned}$$

The sensitivities $y_{\underline{x}_0}$ immediately after the event are given by

$$y_{\underline{x}_0}(\tau^+) = -\left(g^+_y(\tau^+)\right)^{-1} g^+_{\underline{x}}(\tau^+) \underline{x}_{\underline{x}_0}(\tau^+).$$

Following the event, i.e., for $t > \tau^+$, calculation of the sensitivities proceeds according to (19),(20), until the next event is encountered. The jump conditions provide the initial conditions for the post-event calculations.

Hybrid systems usually involve many discrete events. The more general case follows naturally though, and is presented in [5].